Journal of Solid State Chemistry **156,** 237–241 (2001)
doi:10.1006/jssc.2000.8994, available online at http://www.idealibrary.com on IDEAL®

Phase Equilibrium of the La–Ca–Mn–O System

Y. X. Wang, Y. Du, R. W. Qin, B. Han, J. Du, and J. H. Lin[1]

The State Key Laboratory for Rare Earth Materials Chemistry and Applications, Department of Materials Chemistry, Peking University, Beijing 100871, People's Republic of China

Received May 8, 2000; in revised form September 20, 2000; accepted October 6, 2000; published online December 21, 2000

Phase equilibrium of the La–Ca–Mn–O system at 900°C in atmosphere was examined and illustrated in the form of a phase diagram. $La_{1-x}Ca_xMnO_3$ forms a solid solution with two distinct perovskite structures ($R\bar{3}c$ and *Pnma*). A new compound $La_2Ca_2MnO_7$, identified in the phase diagram, crystallizes in a rhombohedral structure ($R\bar{3}$) with the lattice constants of $a = 5.62176(4)$, $c = 17.3161(2)$ Å. The phase regions in the La–Ca–Mn–O system were clarified based on the X-ray diffraction analysis of the samples. © 2001 Academic Press

Key Words: **La–Ca–Mn–O system; phase relation.**

INTRODUCTION

Rare earth and alkaline earth manganates have been the subjects of numerous papers because of their extraordinary physical properties, such as colossal magnetoresistance (CMR) (1–3). Despite the long history of work on these materials, there have been few systematic investigations of the phase equilibrium across the full range of the systems. The phase equilibrium of manganate systems is complicated by the fact that the oxidation state of manganese may vary in different compounds. A slight change of the synthetic condition often yields completely different products; thus the knowledge of phase equilibrium is required both for rational synthesis of the manganese oxides and for exploiting unknown phases in these systems. In the present report, we focus on an isothermal section of the La–Ca–Mn–O system at 900°C in atmosphere.

The binary sections in the La–Ca–Mn–O system have been studied extensively. It was mentioned that a ternary compound La_2CaO_4 forms between 850 and 1000°C (4) in the La–Ca–O system, but no further confirmation was reported. In the La–Mn–O system (5–10), three compounds, La_2MnO_4, $LaMnO_3$, and $LaMn_7O_{12}$, were known. La_2MnO_4, crystallized in the $KNiF_4$ structure, is formed only at low oxygen partial pressure (6). $LaMnO_3$ crystallizes in the perovskite structure and forms a solid solution from La/Mn = 0.908 to 1.202 at 850°C; at high temperature (1127°C) the solid solution reduces to La/Mn = 0.91 to 1.10 (4). It has been known that $LaMnO_3$ is a cation-deficient compound (7–9), and it was expressed as a nonstoichiometric phase $La_{0.94}Mn^{3+}_{0.745}Mn^{4+}_{0.235}O_3$ by Tofield *et al.* (9). $LaMn_7O_{12}$ is a high-pressure phase and was obtained under 40 kbar at 1000°C. It crystallizes also in a perovskite-related structure (ABO_3) where La^{3+} and part of Mn^{3+} are ordered in the *A*-sites and Mn^{4+} and the rest of Mn^{3+} locate randomly at the *B* sites (10).

The Ca–Mn–O system (11) consists of a number of compounds. The phases that are stable in air include Ca_2MnO_4 (<1600°C), $Ca_3Mn_2O_7$ (<1500°C), $Ca_4Mn_3O_{10}$ (<1480°C), $CaMnO_3$ (<1400°C), $CaMn_2O_4$ (<1400°C), $CaMn_3O_6$ (<860°C), $CaMn_4O_8$ (<810°C), and $CaMn_7O_{12}$ (<940°C). Most of these phases crystallize in perovskite-related structures. $CaMnO_3$ is a typical perovskite with orthorhombic symmetry. Ca_2MnO_4, $Ca_3Mn_2O_7$, and $Ca_4Mn_3O_{10}$ are, respectively, the $n = 1$ to 3 members of the Ruddlesden–Popper family $A_{n+1}B_nO_{3n+1}$ (12). The structure of $CaMn_7O_{12}$ is similar to that of $LaMn_7O_{12}$ (10). The structures of the other two compounds, $CaMn_3O_6$ and $CaMn_4O_8$, remain unknown.

For the pseudoternary La_2O_3–CaO–MnO_x system, most of studies were focused on the solid solution $La_{1-x}Ca_xMnO_3$ and the Ruddlesden–Popper phase of $La_xCa_{3-x}Mn_2O_7$ ($n = 2$), because of their giant magnetoresistivity (GMR) properties. $La_{1-x}Ca_xMnO_{3+\delta}$ crystallizes in distorted perovskite structure. Shuk *et al.* (13) and Mahendrian *et al.* (14) both indicated that $La_{1-x}Ca_xMnO_3$ has rhombohedral structure for $x < 0.2$ and becomes cubic for $x > 0.2$. However, a recent study by Faaland *et al.* (15) on $La_{1-x}Ca_xMnO_3$ ($x = 0.2$ to 0.6) prepared at 1000°C indicated that the structure is orthorhombic with space group *Pnma*. In addition, Murakami *et al.* (16) observed superreflection at 107 K, and they attributed this observation to the charge ordering of Mn^{3+} and Mn^{4+} in the materials. A complete magnetic phase diagram study (17) shows that $La_{1-x}Ca_xMnO_3$ is a ferromagnetic insulator for $x < 0.18$ and becomes a

[1]To whom correspondence should be addressed. Fax: (8610) 62751708. E-mail: jhlin@chem.pku.edu.cn.

0022-4596/01 $35.00

ferromagnetic metal for $0.18 < x < 0.5$; further substitution of Ca ($x > 0.5$) induces a transformation to antiferromagnetic insulator. The Ruddlesden–Popper phase $La_xCa_{3-x}Mn_2O_7$ also forms a solid solution (18). Recent structural characterization shows that the $LaCa_2Mn_2O_7$ crystallizes in orthorhombic structure (*Cmcm*), in which double perovskite layers and rock salt layers alternate along the *c*-axis. Nevertheless, formation of this phase is slow, and it can only be obtained by extensive heating at 1350°C for 28 days.

Despite the wealth of physical and chemical information on the phases in the La–Ca–Mn–O system, the relationship between the phases was not clear. The aim of the present work was to investigate the phase relationship in the La–Ca–Mn–O system. Considering the stable range of the corresponding ternary phases, we focus on the phase equilibrium at 900°C.

EXPERIMENTAL

Samples in the La–Ca–Mn–O system were prepared by means of the citrate/nitrate method (19). For a typical reaction, stoichiometrical $La(NO_3)_3$, $Mn(NO_3)_2$, and $Ca(NO_3)_2$ were dissolved in water and excess citric acid was added. The solution was heated on a hot plate with stirring until the combustion reaction was completed. The obtained black oxide precursor was ground and heated at 600°C in a furnace for 2 h in air and then at 900°C for 48 h. All samples were air-quenched from 900°C to room temperature.

X-ray powder diffraction patterns were obtained using a Rigaku D/Max-2000 diffractometer with Cu$K\alpha$ radiation. Rietveld refinements, using the GSAS program (20), were performed for $La_2Ca_2MnO_7$ and the $La_{1-x}Ca_xMnO_3$ system. Chemical analysis of the cations was performed by inductively coupled plasma atomic emission spectroscopy, and the formal oxidation state of manganese was analyzed using the oxalate titration method for $La_2Ca_2MnO_7$.

RESULTS AND DISCUSSION

Phase Relations in the La–Ca–Mn–O System

The citric complexes were known to be suitable precursors for synthesis of complex oxides at relatively low temperature (19). The combustion of the citric complexes often leads to fine oxide powders, which significantly reduces the diffusion length of the reactant species, so that the equilibrium of the system can be reached in a relatively short time. This technique has been widely used in the synthesis of superconductive copper oxides and other oxide systems. For the La–Ca–Mn–O system, the phase equilibrium can be reached within 2 days at 900°C by using this method. The evidence that equilibrium was established under such conditions was that all of the known ternary compounds were obtained as single phases.

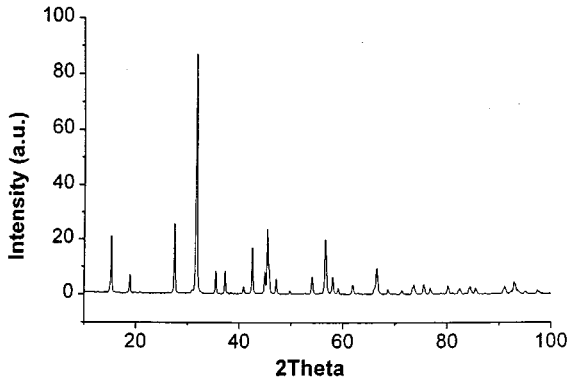

FIG. 1. X-ray powder diffraction pattern of $La_2Ca_2MnO_7$.

In the La–Mn–O system, the perovskite compound $LaMnO_3$ forms a solid solution from La/Mn = 1.22 to 0.90 at 900°C, which agrees with observations by van Roosmalen *et al.* (6). In the Ca–Mn–O system, six compounds, $CaMnO_3$, Ca_2MnO_4, $Ca_3Mn_2O_7$, $Ca_4Mn_3O_{10}$, $CaMn_2O_4$, and $CaMn_7O_{12}$, were identified. The other two known phases, $CaMn_3O_6$ and $CaMn_4O_8$, did not appear because the reaction temperature in our experiment was beyond their decomposition temperature. In the La–Ca–O system, we did not observe any indication of the presence of La_2CaO_4.

In the pseudoternary system La–Ca–Mn–O, all of the samples in the $La_{1-x}Ca_xMnO_3$ ($0 < x < 1$) system were identified as single phases with perovskite-type structure. The symmetry of the structure varies from rhombohedral ($0 < x < 0.1$) to orthorhombic ($x \geq 0.1$). In the present study, we did not intend to synthesize the solid solution of the Ruddlesden–Popper phase $La_xCa_{3-x}Mn_2O_7$ (18) because that formation of this phase is kinetically slow at 900°C. However, a new compound with composition $La_2Ca_2MnO_7$ was identified in the La–Ca–Mn–O system. Figure 1 shows the X-ray diffraction pattern of $La_2Ca_2MnO_7$. $La_2Ca_2MnO_7$ crystallizes in a rhombohedral structure ($R\bar{3}$) with lattice constants of $a = 5.62176$ (4), $C = 17.3161$ (2) Å. Table 1 lists the reflection indexes of this compound. The crystal structure of $La_2Ca_2MnO_7$ has been solved by using the direct method and refined with the Rietveld method on both X-ray and neutron diffraction powder data that has been published elsewhere (21). The structure of $La_2Ca_2MnO_7$ can be described as a hexagonal perovskite intergrowth compound with alternate stacking of single-hexagonal perovskite layers (La_2MnO_6) and "Ca_2O" layers (21). In Fig. 2 we summarize the observed compounds in the La–Ca–Mn–O system.

To construct the phase diagram, more than 80 samples in the La–Ca–Mn–O system were synthesized and examined by X-ray powder diffraction. Figure 3 shows the distribution of the tested compositions in the La–Ca–Mn–O system.

TABLE 1
Indexes of X-Ray Powder Reflections of $La_2Ca_2MnO_7$

h	k	l	2θ (calc)	2θ (exp)	d (Å) (exp)	I/I_0
0	0	3	15.34	15.33	5.776	22
1	0	1	18.93	18.91	4.689	7
1	0	−2	20.93	20.90	4.246	<1
1	0	4	27.56	27.55	3.235	29
0	0	6	30.97	30.90	2.892	2
1	0	−5	31.69	31.78	2.813	100
2	−1	0	31.83			
2	−1	3	35.51	35.49	2.527	10
2	0	−1	37.29	37.28	2.410	10
2	0	2	38.40	38.30	2.348	<1
1	0	7	40.90	40.92	2.204	5
2	0	−4	42.59	42.58	2.122	21
2	−1	6	45.00	44.98	2.014	11
2	0	5	45.53	45.50	1.992	40
1	0	−8	45.86	45.84	1.978	11
0	0	9	47.22	47.20	1.924	8
3	−1	1	49.82	49.77	1.830	4
3	−2	−4	54.14	54.11	1.694	9
3	−1	5	56.62	56.64	1.624	27
2	−1	−9	58.07	58.05	1.588	9
3	0	3	59.11	59.07	1.563	5
1	0	−11	61.92	61.90	1.498	5
4	−2	0	66.51	66.50	1.405	12
4	−2	3	68.71	68.72	1.365	5

Note. The space group of the structure is $R\bar{3}$ and the refined lattice constants are $a = 5.62176$ (4), $c = 17.3161$ (2) Å.

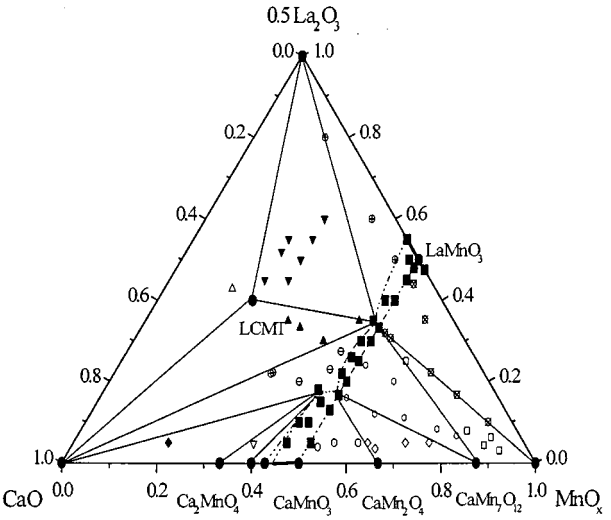

FIG. 3. Distribution of the tested samples in different phase regions of the La–Ca–Mn–O system; LCMT represents the quaternary phase of $La_2Ca_2MnO_7$; the symbols in the diagram represent the following coexisting phases: (■) solid solution around $La_{1-x}Ca_xMnO_3$ $(0 < x < 1)$, (⊗) $La_{1-x}Ca_xMnO_3$ $(0 < x \le 0.33) + Mn_3O_4$, (□) $La_{0.67}Ca_{0.33}MnO_3 + Mn_3O_4 + CaMn_7O_{12}$, (○) $La_{1-x}Ca_xMnO_3$ $(0.33 \le x \le 0.67) + CaMn_7O_{12}$, (◇) $La_{0.33}Ca_{0.67}MnO_3 + CaMn_2O_4 + CaMn_7O_{12}$, (⊙) $La_{1-x}Ca_xMnO_3$ $(0.67 \le x < 1) + CaMn_2O_4$, (▽) $La_{0.33}Ca_{0.67}MnO_3 + Ca_2MnO_4 + Ca_3Mn_2O_7$, (◆) $La_{0.33}Ca_{0.67}MnO_3 + Ca_2MnO_4 + CaO$, (⊖) $La_{1-x}Ca_xMn_1O_3$ $(0.33 \le x \le 0.67) + CaO$, (▲) $CaO + La_2Ca_2MnO_7 + La_{0.67}Ca_{0.33}MnO_3$, (△) $CaO + La_2O_3 + La_2Ca_2MnO_7$, (▼) $La_2O_3 + La_2Ca_2MnO_7 + La_{0.67}Ca_{0.33}MnO_3$, (⊕) $La_2O_3 + La_{1-x}Ca_xMnO_3$ $(0 < x \le 0.33)$.

The fundamental components, CaO and La_2O_3, appeared as rock salt and the A-type Ln_2O_3 structure, respectively, in the system. Manganese oxide was known (11, 22, 23) to be present as Mn_2O_3 at lower temperature; it converts to Mn_3O_4 in air at 871°C (22). Another form of manganese oxide γ-Mn_2O_3 (black) can be obtained by careful dehydration of hydrated manganese sesquioxide in vacuum at 250°C (23). Both Mn_3O_4 and γ-Mn_2O_3 crystallize in a distorted spinel structure (24). In the present study, manganese oxide was found in the spinel structure, and the purplish-red color indicates that it was indeed the Mn_3O_4 (23, 24). However, the oxidation state of manganese in other compounds of the system depends strongly on the crystal structure. Therefore, the phase diagram presented here is an equilibrium diagram of the La–Ca–Mn–O system at a certain temperature (900°C) and oxygen partial pressure ($P_{O_2} = 0.21$ atm). For example, the tie line between Mn_3O_4 and $LaMnO_3$ is a pseudobinary system, in which manganese presents in both 3+ and 2+. Nevertheless, as shown in Fig. 4, most of the phase regions in the La–Ca–Mn–O system are clearly defined under the present experimental conditions.

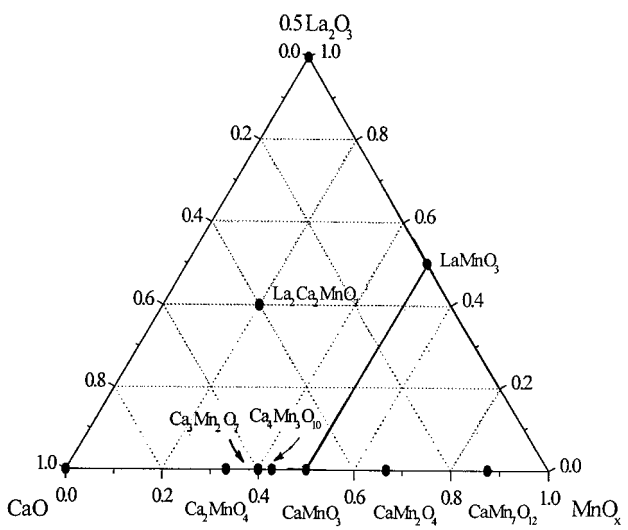

FIG. 2. Distribution of the compounds in the La–Ca–Mn–O system at 900°C in air.

The phase diagram of the La–Ca–Mn–O system is essentially divided into two regions by the solid solution of $LaMnO_3$–$CaMnO_3$. In principle, the $LaMnO_3$–$CaMnO_3$ should contain a two-phase region, because the two distinct perovskite structures were observed. In the present study, we only observed a gradual merge of some reflections when

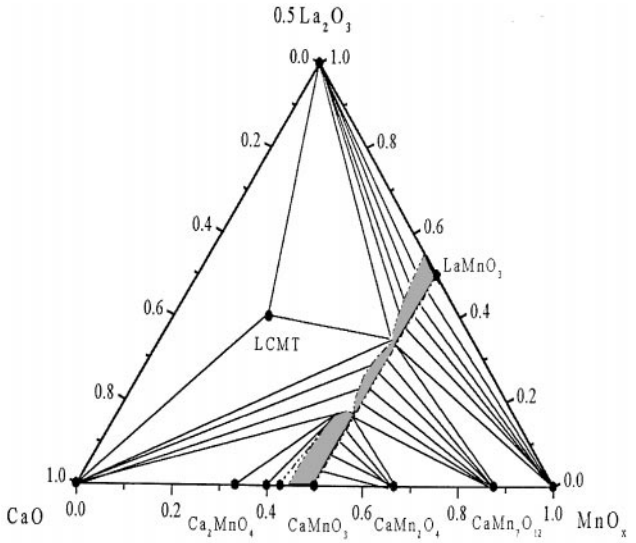

FIG. 4. Phase relationship at 900°C in the La–Ca–Mn–O system; LCMT represents the quaternary phase of $La_2Ca_2MnO_7$; the shaded region represents the solid solution of $La_{1-x}Ca_xMnO_3$, the lineate regions are two-phase regions, and the blank regions represent three-phase regions in the system.

the structure changed from rhombohedral to orthorhombic, indicating that the two-phase region is narrow. As an approximation, the $LaMnO_3$–$CaMnO_3$ system might be considered as a complete solid solution, and in this sense, the La–Ca–Mn–O system could be divided into two parts, $LaMnO_3$–$CaMnO_3$–Mn_3O_4 and CaO–La_2O_3–$LaMnO_3$–$CaMnO_3$.

As shown in Fig. 4, two three-phase regions and three two-phase regions were identified in the $LaMnO_3$–$CaMnO_3$–Mn_3O_4 part. In the CaO–La_2O_3–$LaMnO_3$–$CaMnO_3$ system, at least four three-phase regions have been clearly identified. The phase regions around Ca_2MnO_4 and $CaMnO_3$ are not clearly defined, because the X-ray diffraction patterns of the Ruddlesden–Popper compounds

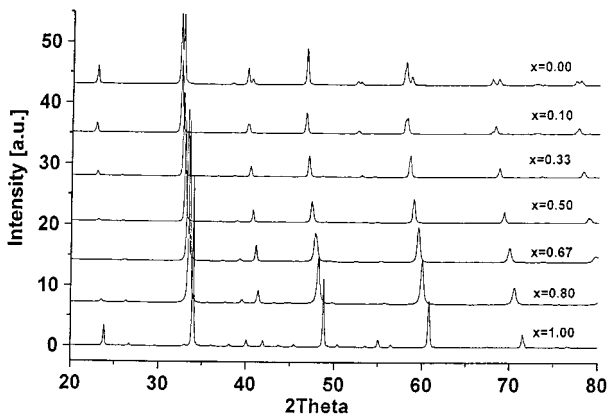

FIG. 5. X-ray powder diffraction patterns of the samples in the $La_{1-x}Ca_xMnO_3$ system; the compositions of the samples are indicated in the figure.

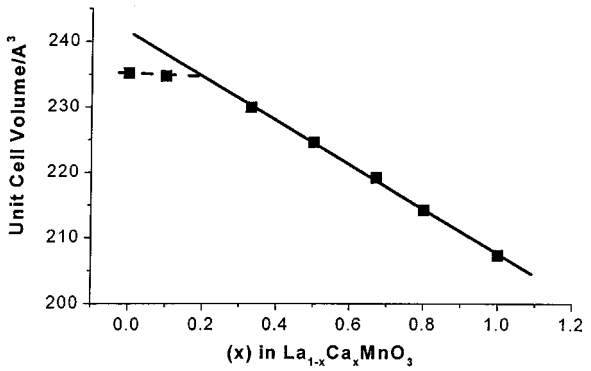

FIG. 6. The composition dependence of the unit cell volumes in the $La_{1-x}Ca_xMnO_3$ system.

($La_xCa_{3-x}Mn_2O_7$ and $La_xCa_{4-x}Mn_3O_{10}$) are rather similar to those of the ternary phases ($Ca_3Mn_2O_7$ and $Ca_4Mn_3O_{10}$). The boundaries of these regions are, therefore, represented by dotted lines in Fig. 4. The lineate regions in the figure are the two-phase regions composed of the perovskite solid solution and the corresponding compounds. $La_2Ca_2MnO_7$ is a sharp line-compound, and no solid solution was found around this composition.

$La_{1-x}Ca_xMnO_3$ Solid Solution

All of the samples in the solid solution $La_{1-x}Ca_xMnO_3$ obtained at 900°C in air have the perovskite structure. The $LaMnO_3$ crystallizes in rhombohedral perovskite structure with lattice constants of $a = 5.5242$ (1) and $c = 13.3476$ (4) Å. The solid solution of $La_{1-x}Mn_{1-y}O_3$ seems to retain the rhombohedral structure in a region from La/Mn = 1.22 to 0.90. The structure refinement on a typical $LaMnO_3$ sample indicates that the La position is partially occupied with an occupation factor of 0.971 (4), which is comparable to the result of Tofield *et al.* (9).

A small amount of Ca substitution induces a structure change from rhombohedral to orthorhombic in the $La_{1-x}Ca_xMnO_3$ system (13–15), which can be visualized from the X-ray powder diffraction patterns shown in Fig. 5. The diffraction pattern of the hexagonal $LaMnO_3$ is characterized by splitting of $(2\bar{1}0)$ and $(1\,0\,4)$ at about $2\theta = 32.5°$, which merges into more or less a single peak in the orthorhombic form. Figure 6 shows variation of the unit cell volume of the $La_{1-x}Ca_xMnO_3$ system; it is a straight line in the orthorhombic region but deviates in the rhombohedral region ($x = 0.1 \sim 0.33$). The hexagonal $LaMnO_3$ was known to contain a considerable amount of cation vacancies (9); the deviation from Vegard's law in the rhombohedral region of the $La_{1-x}Ca_xMnO_3$ system is largely due to the contraction effect of the cation vacancy. Substitution of La by Ca stabilizes orthorhombic structure, and the minimum substitution for stabilizing the orthorhombic structure is around $x = 0.1 \sim 0.33$. We synthesized

TABLE 2
Cell Parameters and Refined Residual Values of $La_{1-x}Ca_xMnO_3$ (900°C, in Air)

X	Phase composition	Unit cell parameters				Space group	R_p
		a (Å)	b (Å)	c (Å)	V (Å^3)		
0.00	$LaMnO_3$	5.5242 (1)	—	13.3476 (4)	352.76	*R*–3*m*	0.065
0.10	$La_{0.9}Ca_{0.1}MnO_3$	5.4823 (1)	7.7593 (2)	5.5172 (1)	234.70	*Pnma*	—
0.33	$La_{0.67}Ca_{0.33}MnO_3$	5.4557 (5)	7.7201 (11)	5.4581 (6)	229.89	*Pnma*	0.073
0.50	$La_{0.5}Ca_{0.5}MnO_3$	5.4118 (9)	7.6732 (3)	5.4080 (9)	224.57	*Pnma*	0.087
0.67	$La_{0.33}Ca_{0.67}MnO_3$	5.3679 (18)	7.6168 (5)	5.3607 (18)	219.18	*Pnma*	0.086
0.80	$La_{0.20}Ca_{0.80}MnO_3$	5.3338 (6)	7.5236 (4)	5.3381 (5)	214.22	*Pnma*	0.080
1.00	$CaMnO_3$	5.2802 (2)	7.4562 (4)	5.2657 (2)	207.31	*Pnma*	0.10

several samples around $x = 0.1 \sim 0.33$, but no two-phase region was observed. It is likely that the two-phase region is too narrow to be detected experimentally. Table 2 lists the lattice constants and the residual values of the structure refinement in the $La_{1-x}Ca_xMnO_3$ system. The structure refinements of the phases of $x \geq 0.1$ show that all of the phases in this region crystallize in the orthorhombic perovskite structure in the space group of *Pnma*, and the refined La/Ca ratios fit nicely with those of the initial compositions.

The solid solution region around $La_{1-x}Ca_xMnO_3$ were examined by varying (La, Ca)/Mn ratios. As shown in Fig. 4, the solid solution of the orthorhombic phase (Ca-rich part) in $La_{1-x}Ca_xMnO_3$ extends to the Mn-deficient side, and no significant extension to the Mn-rich side has been observed. This is similar to $Ca_{1-x}MnO_3$, but different from that of the La-rich part, where the solid solution extends to both sides near $LaMnO_3$.

In conclusion, the La–Ca–Mn–O system at 900°C in air consists of more compounds; therefore, the phase diagram is more complicated in comparison with the La–Sr–Mn–O system (25). In La–Sr–Mn–O, $La_{1-x}Sr_xMnO_3$ contains a wide two-phase region. The two-phase region is not detectable in $La_{1-x}Ca_xMnO_3$, though a symmetry change of the structure from rhombohedral to orthorhombic did appear. In addition, a hexagonal perovskite-intergrowth compound $La_2Ca_2MnO_7$ was found in the La–Ca–Mn–O system, and the corresponding compound of $La_2Sr_2MnO_7$ does not exist in the La–Sr–Mn–O system.

ACKNOWLEDGMENTS

The authors thank Professor Tian of Peking University for stimulating discussions. Financial support from the NSFC (29625101 and 29731010) and the State Key Basic Research Program is gratefully acknowledged.

REFERENCES

1. R. von Helmolt, J. Wecker, B. Holzapfel, L. Schultz, and K. Samwer, *Phys. Rev. Lett.* **71** (14), 2331 (1993).
2. C. N. R. Rao, A. K. Cheetham, and R. Mahesh, *Chem. Mater.* **8,** 2421 (1996).
3. B. Raveau, A. Maignan, C. Martin, and M. Hervieu, *Chem. Mater.* **10,** 2641 (1998).
4. B. Acharya, J. Muralidhar, and L. R. Pradham, Regional Research Lab, Orissa, India, ICDD Grant-in-Aid, 1991. [See JCPDS 42-0342]
5. J. A. M. van Roosmalen, P. van Vlaanderen, E. H. P. Cordfunke, W. I. Ijdo, and D. J. W. Ijdo, *J. Solid State Chem.* **114,** 516 (1995).
6. M. L. Borlera and F. Abbattista, *J. Less-Common Met.* **92,** 55 (1995).
7. J. A. M. van Roosmalen and E. H. P. Cordfunke, *J. Solid State Chem.* **110,** 109 (1994).
8. P. Norby, I. G. K. Andersen, and E. K. Andersen, *J. Solid State Chem.* **119,** 191 (1995).
9. B. C. Tofield and W. R. Scott, *J. Solid State Chem.* **10,** 183 (1974).
10. B. Bochu, J. Chenevas, J. C. Joubert, and M. Marezio, *J. Solid State Chem.* **11,** 88 (1974).
11. H. S. Horowitz and J. M. Longo, *Mater. Res. Bull.* **13,** 1359 (1978).
12. S. N. Ruddlesden and P. Popper, *Acta Crystallogr.* **11,** 541 (1958).
13. L. Tichonova Shuk and U. Guth, *Solid State Ionics* **68,** 177 (1994).
14. Mahendiran, S. K. Tiwary, A. K. Raychaudhuri, T. V. Ramakrishnan, R. Mahesh, N. Ranggavittal, and C. N. R. Rao, *Phys. Rev. B* **53,** 3348 (1996).
15. Faaland, K. D. Knudsen, M.-A. Einarsrud, L. Rørmark, R. Høier, and T. Grande, *J. Solid State Chem.* **140,** 320 (1998).
16. Y. Murakami, D. Shindo, H. Chiba, M. Kikuchi, and Y. Syono, *J. Solid State Chem.* **140,** 331 (1998).
17. P. Schiffer, A. P. Ramirez, W. Bao, and S. W. Cheong, *Phys. Rev. Lett.* **75,** 3336 (1995).
18. M. A. Green and D. A. Neumann, *Chem. Mater.* **12,** 90 (2000); P. Raychaudhuri, C. Mitra, A. Paramekanti, R. Pinto, A. K. Nigam, and S. K. Dhar, *J. Phys. Condens. Matter* **10,** L191 (1998); H. Asano, J. Hayakawa, and M. Matsui, *Appl Phys. Lett.* **68,** 3638 (1996); H. Asano, J. Hayakawa, and M. Matsui, *Phys. Rev. B Condens. Matter* **56,** 5395 (1997); H. Asano, J. Hayakawa, and M. Matsui, *Appl. Phys. Lett.* **70,** 2303 (1997); H. Asano, J. Hayakawa, and M. Matsui, *Jpn. J. Appl. Phys. 1 Lett.* **36,** L104 (1997).
19. C. Marcilly, P. Courty, and B. Delmon, *J. Am. Ceram. Soc.* **53,** 56 (1970).
20. C. Larson and R. B. von Dreele, Report LAUR 86–748, Los Alamos National Laboratory, 1985.
21. Y. X. Wang, J. H. Lin, Y. Du, R. W. Qin, B. Han, and C. K. Loong, *Angew. Chem.* **112,** 2842 (2000); *Angew. Chem. Int. Ed. Engl.* **112,** 2730 (2000).
22. E. M. Otto, *J. Electrochem. Soc.* **111,** 88 (1964).
23. T. E. Moore, M. Ellis, and P. W. Selwood, *J. Am. Chem. Soc.* **72,** 856 (1950).
24. A. F. Wells, "Structural Inorganic Chemistry," 5th ed., pp. 553–554. Clarendon, Oxford, 1984.
25. V. A. Cherepanov, L. Y. Barkhatova, and V. I. Voronin, *J. Solid State Chem.* **134,** 38 (1997).